# NUMERICAL AND EXPERIMENTAL EVALUATION OF THE DRYING BEHAVIOUR OF MEDIUM DENSITY EXPANDED CORK BOARDS USED AS AN EXTERNAL COATING

R. FINO[1], N. SIMÕES[1,2] & A. TADEU[1,2]
[1]ITeCons; Coimbra, Portugal.
[2]Department of Civil Engineering; University of Coimbra, Coimbra, Portugal.

ABSTRACT

The promotion of more efficient and greener buildings and the reduction of energy consumption are among the priorities defined in the Europe 2020 Strategy. The potential of incorporating different types of waste and by-products in construction materials and solutions is relevant for achieving a more sustainable construction and use of buildings throughout their life cycle. Example of this, is the use of the medium density insulation cork board (MD ICB) as an external insulation coating material. It is a fully natural and recyclable insulation material, made from the exudation of cork granules, a sub-product from the cork industry. This material is sensitive to rain conditions as it absorbs water. When the energy performance of buildings is being assessed, the influence of moisture on its thermal behaviour should not be neglected. A building's heat loss estimation can be far from reality if the materials' moisture content is not considered. Therefore, it is of crucial importance to evaluate the drying behaviour of MD ICB after wetting this material. A numerical simulation, using WUFI 2D 3.0 was performed to evaluate the materials' moisture content over time. In order to perform this study a thorough experimental characterisation of the material, in terms of hygrothermal parameters, was required. To validate the numerical model, the obtained numerical results were compared with experimental ones, in which MD ICB boards were dried in a climatic chamber, after being saturated with water. After the first 9 hours of drying, during which the moisture movement is mostly due to gravity, the experimental and numerical results present relatively good correlation.

*Keywords: cork, hygrothermal parameters, insulation materials, mass transfer, evaluation, numerical simulation.*

## 1 INTRODUCTION

Cork is a natural resource that grows without chemical herbicides, fertilizers or irrigation, which is also renewable. Cork comes from the outer layers of the bark of the Quercus Suber L., a type of oak tree that is native to the western Mediterranean region. Cork is an organic, light and natural product. It is dimensionally stable and presents considerable resistance to compression loads. These features make cork suitable to be used in a wide spectrum of applications [1]. Insulation cork board is obtained from the exudation of cork granules by the action of water steam [2]. An important advantage of insulation corkboard is its resistance to chemical and biological agents[3] and the ability to maintain its physical properties at lower temperatures compared to other insulator materials (cork working range −180 to 110°C) [4], and for longer period of times. Gil and Silva [5] studied ICB obtained from demolitions, with several decades of intensive use, and concluded that ICB maintained a

WIT CONFERENCES

This paper is part of the Proceedings of the 6th International Conference on Harmonisation between Architecture and Nature (Eco-Architecture 2016)
www.witconferences.com


ISSN: 1743-7601 (paper format), ISSN: 1743-761X (online), http://www.witpress.com/journals
DOI: 10.2495/SDP-V12-N2-315-325

great thermal behaviour and that most of the mechanical properties align to standard values, proving material durability.

To obtain a more accurate building thermal behaviour, a moisture migration analysis in building walls should be carried out [6–8]. Neglecting the moisture dependence of heat and moisture transport parameters in any energy-related assessment of a building, in particular for thermal insulation materials (TIM), can induce results in heat loss estimation, which can be far from the real values [6]. A qualitative overview of traditional TIM was presented by Jelle [9]. In this work it can be seen that the TIM thermal conductivities (λ [W/mK]) are sensitive to temperature, moisture content and mass density. The role of moisture content in TIM is highlighted, since thermal conductivity increases significantly when moisture content increases. Srinivasan, and Wijeysundera [10], conclude that, under several driving forces, the moisture transport in cork slabs is more due to thermal diffusion rather than due to evaporation/condensation mechanisms, since equilibrium humidity is lower in cold regions, as moisture migrates from hot to cold regions [10–12]. Therefore, in winter, when the outer face of the material is colder, the vapour migrates to the outer building envelope. In summer, the opposite occurs, but the transport of water molecules is faster as the temperature is higher, because connections can be released more easily, decreasing the amount of water adsorbed by the material [6].

MD ICB is a material that has been developed to be used as an external thermal insulation coating. Considering that there are no technical or architectural constraints, the exterior thermal insulation of facades have several advantages, such as the reduction of thermal bridges and the maintenance of thermal inertia. However, since the material is exposed to the elements, it will absorb water. The aim of this study is to evaluate the MD ICB drying behaviour over time, after the material has been wetted. For this purpose, a thorough experimental characterisation of the material, in terms of hygrothermal parameters, was performed. To validate the numerical model, the drying process of the material, after being wet, was experimentally studied and its results compared with the numerical ones. Numerical simulations were performed using WUFI 2D 3.0 [13].

## 2 EXPERIMENTAL CHARACTERISATION OF THE MATERIAL

To perform numerical simulations, it is necessary to insert data on the material properties. Those properties as well as the experimental procedures to obtain them, are succinctly described in the next sections. Unless otherwise be said, the test specimens (TS) have the nominal dimensions of (300 × 300 × 70) $mm^3$.

### 2.1 MD ICB basic properties

#### 2.1.1 Bulk Density, porosity and specific heat capacity (dry)

To find the bulk density [$kg/m^3$] of MD ICB, 15 TS were used. The procedures described on EN 1,602:2013 [14] were adopted. For porosity [$m^3/m^3$], 6 TS with nominal dimensions of (150 × 150 × 60) were used. The procedures described on NP EN 1936:2008 [15] were applied. The specific heat capacity in dry state [J/kg.K] was calculated using the 'Ratio method'.

#### 2.1.2 Thermal conductivity in dry state

For a homogenous material, thermal conductivity (λ) is defined as a heat quantity, by time unit, which flows through a layer with unitary thickness and area, for unitary temperature difference between the two faces of the material [16]. 15 TS were used. They were dried on

a ventilated oven until constant in mass. To avoid any moisture absorption, each one of the TS was placed in a thin plastic bag. The procedures described by NP EN 12667 [16] were applied. The apparatus used was an NETZSCH HFM 436/3/1 Lambda.

2.1.3 Free saturation water content mass by volume [kg/m$^3$]

A capillary-active material in contact with water will absorb it until free saturation is reached. This water content, $\psi_{sat}$ [kg/m$^3$], corresponds to the moisture storage function at a relative humidity of 1 (= 100%) [13]. Because of air pockets trapped in the pore structure, the free saturation water content is less than the maximum water content, $\psi_{max}$. To calculate $\psi_{sat}$, 5 TS were used. They were immersed in water for 72 hours. After this time, the TS were removed from water and their mass was recorded. Then the TS were dried in a ventilated oven until constant mass was achieved. Saturation water content, mass by volume [kg/m$^3$] was calculated using eqn (1).

$$\psi_{sat} = u \frac{\rho_0}{\rho_w} \text{ [kg / m}^3\text{]} \quad (1)$$

Where $u$ is the water content mass by mass, calculated using eqn (2), $\rho_0$ is the density of the dry material and $\rho_\omega$ is the density of water at 23°C and equal to 997.6 kg/m$^3$.

$$u = \frac{m - m_0}{m_0} \text{ [kg / kg]} \quad (2)$$

$m$ is the mass of TS at saturated state while $m_0$ is the mass of TS after drying.

2.2 Water vapour transmission properties

The property most often used for comparison of the 'breathability' of materials, is the resistance to vapour diffusion factor, μ, and, for the numerical simulation, this is the only property required. In spite of this, all the properties listed in EN 12086:2013 [17] were calculated. μ-value is the quotient of the water vapour permeability of air and the water vapour permeability of the material [17]. It indicates the factor by which the vapour diffusion in the material is impeded, as compared to diffusion in stagnant air [13]. Five squared TS with nominal dimension of (100 × 100 × 40) mm$^3$ were used. The TS were placed in a climatic chamber, at (23 ± 2) °C and (50 ± 5) % RH during 8 days. The test condition was Set C, 23–50/93, which means that the temperature was (23 ± 1) °C, the relative humidity in dry state was (50 ± 3) % and relative humidity in humid state was (93 ± 3) % [17]. All the required calculations were made in accordance with EN 12086:2013 [17].

2.3 Water absorption coefficient

$A_w$ [kg/(m$^2$.s$^{0.5}$)], is, by definition, the mass of water absorbed by the area of the TS in contact with water, per square root of time. It is achieved by measuring the change in mass of the TS that has its bottom face in contact with water, over a period of at least 24 h. For its calculation, the procedures preconized on EN ISO 15148:2002 [18], were followed. Three TS were used.

For the calculation of $A_w$, $\Delta m_t$ values, defined as the difference between the mass at each weighting and the initial mass per area, were plotted against the square root of the weighting times, as indicated in EN ISO 15148:2002 [18]. If the obtained graphic is type A, that is, after

an initial period of stabilization, a straight line could be drawn through the values of $\Delta m_t$ plotted against $\sqrt{t}$. This line should be extended to zero time, were it cuts the vertical axis, being $\Delta m'_t$ the value of $\Delta m$ [kg/m$^2$] on the straight line at $t = 0$ [s$^{0.5}$]. The water absorption coefficient, $A_W$ [kg/(m$^2$.s$^{0.5}$)], is calculated using eqn (3).

$$A_w = \frac{\Delta m'_{tf} - \Delta m'_0}{\sqrt{t}} \tag{3}$$

where and $\Delta m'_{tf}$ is the value of $\Delta m$ [kg/m$^2$] on the straight line at the final time $t_f$ [s$^{0.5}$].

## 2.4 Hygroscopic sorption properties

The procedures recommended on ISO 12571:2013 [19] for the determination of hygroscopic sorption properties were followed. For the absorption and desorption, curves were considered at five relative humidities (RH): 30%, 50%, 80%, 90%, and 95% RH. A climatic method chamber was used. Five TS were placed in the climatic chamber, at (23 ± 2) °C with increasing values of RH (adsorption curve), until constant mass, for each condition, was achieved. Its mass was recorded. Constant mass is achieved when relative change in moisture does not increase by more than 0.5% between two consecutive weekly measurements [19]. The procedures were repeated at decreasing RH to plot the desorption curve.

## 2.5 Liquid transport coefficients

The predominant moisture transport mechanism in capillary porous materials is the capillary liquid transport. Although it is basically a convective phenomenon, in the context of building physics it is sufficiently accurate to regard the liquid transport in the pore spaces as a diffusion phenomenon [13]:

$$gw = -Dw(w).grad\, w \cdot \tag{4}$$

in which $gw$ [kg/(m².s)] is the liquid transport flux density, $w$ [kg/m²] is the material moisture content and $D$w[m²/s] is the liquid transport coefficient.

$D$w is generally strongly dependent on the materials' moisture content. If a material water content has a linear increase over the square root of time, the liquid transport can be described by the diffusion formula.

There are two liquid transport coefficients: $D$ws is the liquid transport coefficient for suction and $D$ww, the liquid transport for redistribution.

$Dws$ represents the capillary absorption of water when the imbibing surface is fully wetted. The suction transport is dominated by the larger capillaries, since its lower capillary pressure is more than compensated by its significantly lower resistance to flow. This represents, for example, the rain on a facade. $D$ww describes the distribution of the water absorbed by the material, after the rain has stopped, that is, there is no more water absorption. This corresponds to moisture migration when the wetting is finished. Smaller capillaries dominate the redistribution, once their higher capillary tension drag the water out of the largest capillaries.

The water absorption coefficient, $A$ [kg/m$^2$s$^{0.5}$], is the standard parameter used to describe the capillary suction of a material. The increase of $D$ws with moisture content can be estimated using eqn (5) [20, 21].

$$D_{ws}(w) = 3.8.\left(A_w / \Psi_{sat}\right)^2 .1000^{\Psi/\Psi_{sat}-1} \tag{5}$$

WUFI 2D 3.0 automatically generates the liquid transport coefficients based on eqn (5) and the material values of $\psi_{80}$ (water content [kg/m$^3$] at 80% RH) $\psi_{sat}$ and $A_w$ [13].

## 3 MD ICB DRYING BEHAVIOUR

### 3.1 Experimental study

To evaluate experimentally the drying behaviour of MD ICB, four TS were used. Each one of them were dried on a ventilated oven at (70 ± 5) °C for 72 hours. The TS were measured and its dry mass registered. The dry density was calculated. After that, the TS were placed in a climatic chamber at (23 ± 2) °C and (50 ± 5) % RH (reference condition – RC), until constant mass was achieved, and then weighted. Moisture content, at RC, was calculated.

To consider the most unfavourable drying situation, each TS was sealed, in five faces, with paraffin (Fig. 1). They were placed in the climatic chamber at RC until constant mass was achieved and then weighted. Subsequently, the TS were totally immersed in water. After 72 hours, they were removed from water and placed on a drainer with 45° inclination. They were allowed to drain for 5 minutes, after which excess surface water was removed from each board with paper, and then weighed. Its mass, $m_{72}$ was recorded. They were placed inside a climatic chamber, at RC to dry. Each board was weighted at intervals of 30 minutes for the first 6 hours, every hour for the following 3 hours of drying and at 24 h, 27 h, 30 h, 33 h, 48 h, 72 h, 96 h, 120 h, 168 h, 288 h, 360 h, 456 h, 696 h, 768 h, 1,032 h and 1,200 h.

### 3.2 Numerical simulations

To evaluate the drying behaviour of MD ICB after wetting, a numerical simulation, using WUFI 2D 3.0 [13] was performed. The material properties considered were obtained by following the procedures described in the previous sections. A model of an ICB board with dimensions of (300 × 300 × 70) mm$^3$, sealed with paraffin on its five faces, was constructed

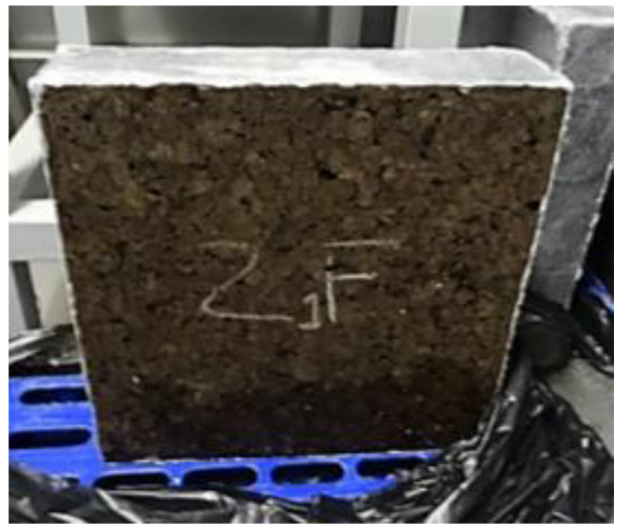

Figure 1: Sealed test specimen.

on WUFI 2D 3.0. The initial conditions were defined. The climate was defined as indoor at a constant temperature of 23°C and 50% RH, to simulate the climate chamber at RC. To validate the model, numerical results were compared with experimental ones.

## 4 RESULTS AND DISCUSSION

### 4.1 Basic properties of MD ICB

Table 1 presents the results obtained for the basic properties of MB ICB.

Table 2 shows the water-vapour tramsmission properties of MD ICB.

### 4.2 Moisture storage and transport coeficients

Figure 2 presents the adsorption and desorption curves of MD ICB. Being a hysteresis notable, the moisture storage function, based on the mean values of absorption and desorption, better defines the moisture storage material behaviour. This function is presented in Table 3.

For the calculation of water absorption coefficient by partial immersion, $A_w$, $\Delta m_t$ values were plotted against the square root of the weighting times, as indicated in EN ISO 15148:2002 [18]. The obtained graph (Fig. 3) is type A, that is, after an initial period of stabilisation, a straight line could be drawn through the values of $\Delta m_t$ plotted against √t.

To calculate the values of $\Delta m'_t$ ($t = 0\ s^{0.5}$) and $\Delta m'_{tf}$ ($t_f = 298\ s^{0.5}$) the correlation lines equations, presented in Fig. 3, for each TS, were used. The obtained values are presented in Table 4, which are the values for $\Delta m'_0$ and $\Delta m'_{tf}$, used to calculate $A_W$.

To calculate the water absorption coefficient, $A_W$ [kg/(m$^2$.s$^{0.5}$)], eqn (3) was used, where $A_W = 0.001433$ [kg/(m$^2$.s$^{0.5}$)].

The moisture transport coefficients, generated by WUFI taking into account the calculated values of $\psi_{80}$, $\psi_{sat}$ and $A_w$, are presented in Table 5.

Table 1: Basic properties of MB ICB.

| Density ρ [kg/m$^3$] | Porosity P [m$^3$/m$^3$] | Specific heat cp [J/kg.K] | Thermal conductivity $\lambda_{10\ dry}$[W/m.K] | Saturation water content $\Psi_{sat}$ [kg/m$^3$] |
|---|---|---|---|---|
| 156 | 0.09 | 1,530 | 0.0413 | 80.64 |

Table 2: Water-vapour transmission properties of MD ICB.

| | Mean value |
|---|---|
| Water vapour transmission rate g [mg/(h.m$^2$)] | 455.54 |
| Water vapour permeance W [mg/(m$^2$.h.Pa)] | 0.33 |
| Water vapour resistance Z [(m$^2$.h.Pa)/mg] | 3.09 |
| Water vapour permeability δ [mg/(m.h.Pa)] | 0.01 |
| Water vapour diffusion resistance factor μ [–] | 54.61 |
| Water vapour diffusion equivalent air layer thickness *Sd* [m] | 2.19 |

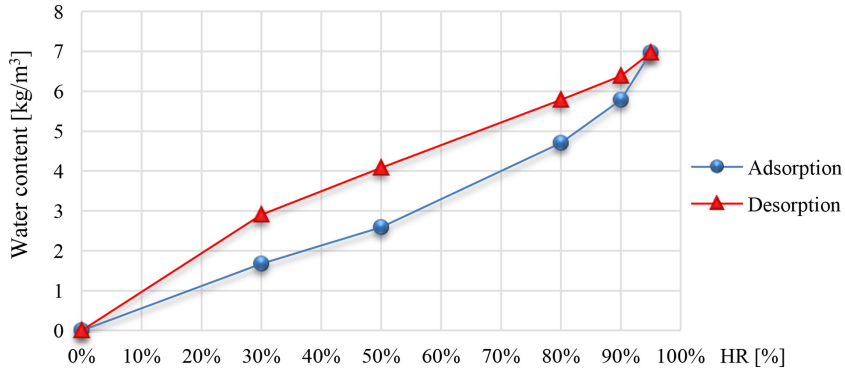


Figure 2: MD ICB adsorption and desorption curve.

Table 3: Moisture storage function of MD ICB, considering the mean values between adsorption and desorption.

| RH [–] | Water content [kg/m$^3$] | RH [–] | Water content [kg/m$^3$] | RH [–] | Water content [kg/m$^3$] |
|---|---|---|---|---|---|
| 0.0 | 0.0 | 0.3 | 2.29 | 0.5 | 3.33 |
| 0.8 | 5.24 | 0.9 | 6.09 | 0.95 | 6.97 |
| 1.0 | 80.64 | | | | |

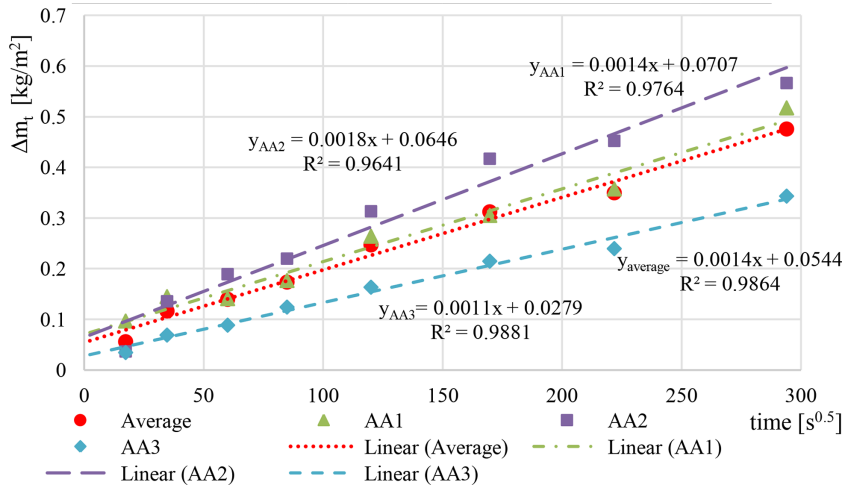


Figure 3: MD ICB water absorption [kg/m$^2$] function of the square root of time [s0.5] and corresponding trend lines. The red dots represent the average values of the 3 TS.

Table 4: $\Delta m_0$ for $t = 0$ [$s^{0.5}$] and $\Delta m_{tf}$ for the final time $t_f$ = 294 [$s^{0.5}$] for each TS and the average values and standard deviation.

| | AA1 | AA2 | AA3 | Average value | σ |
|---|---|---|---|---|---|
| $\Delta m'_0$, t = 0 $s^{0.5}$ | 0.0707 | 0.0646 | 0.0279 | 0.0544 | 0.02 |
| $\Delta m'_{tf}$ t = 294 $s^{0.5}$ | 0.4822 | 0.5937 | 0.3512 | 0.4757 | 0.12 |

Table 5: Moisture transport coefficients automatically generated by WUFI, based on the calculated values of $\psi_{80}$, $\psi_{sat}$ and $A_w$.

| Water content [kg/m$^3$] | *D*ws [m$^2$/s] | *D*ww [m$^2$/s] |
|---|---|---|
| 5.24 | 1.9E-0012 | 1.9E-0012 |
| 80.64 | 1.2E-0009 | 1.2E-0010 |

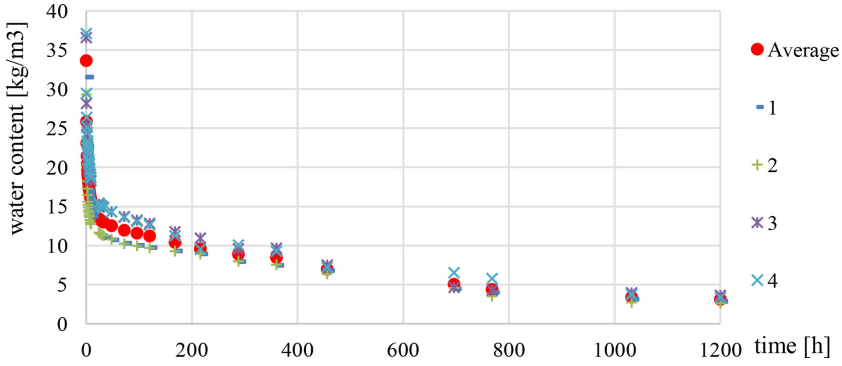


Figure 4: Experimental drying curves for the four TS, from t = 0 to t = 1,200 h. The average value is represented by the red dots.

### 4.3 MD ICB drying behaviour: experimental and numerical study

Figure 4 shows the drying curves of MD ICB, from t = 0 to t = 1,200 h, for each TS. The average value is represented by the red dots.

As can be seen in Fig. 4, in the first hours, the water mass decreases at a very high rate. For a mean initial water content of 33.6 kg/m$^3$, the mean value, at t = 9 h is 15.8 kg/m$^3$. More than half of the initial water content is lost during the first nine hours of drying. As the material presents macro pores, the water retained therein has a tendency to drain rapidly, in liquid state, mainly due to the action of gravity.

Figure 5 presents an ICB board drying in the climatic chamber. Figure 5a shows the MD ICB board at t = 3 h. It is clearly visible that the water accumulation at the bottom of the board, is due to gravity. At t = 9 h, the water at the bottom has almost disappeared. The drying process is now mainly due to capillary conduction and surface diffusion. For that reason, the

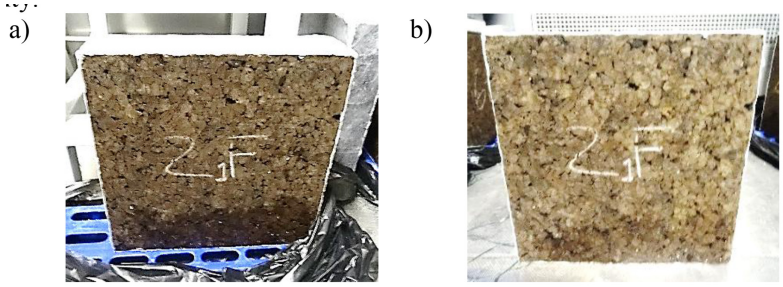


Figure 5: MD ICB board drying at climatic chamber: (a) t = 3 h; (b) t = 9 h.

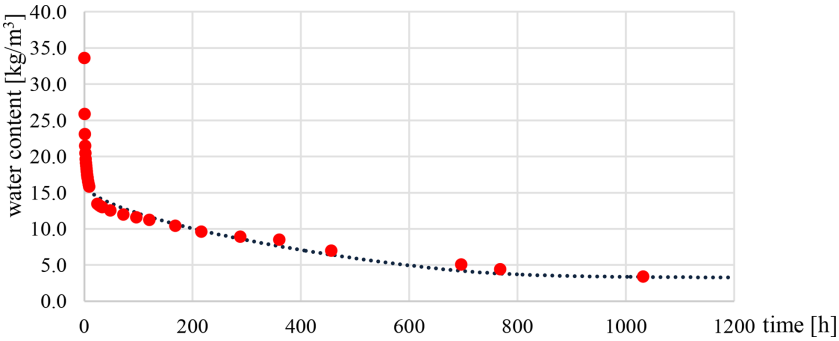


Figure 6: Drying: experimental results from t = 0 until t = 1,200 h (red dots); numerical results (blue dotted line), from t = 9 h until t = 1,200 h, considering an initial water content of 15.8 kg/m$^3$.

numerical simulation was performed assuming, as a starting point, the material condition after the first 9 hours; therefore, $\psi$= 15.8 kg/m$^3$. The obtained curve is presented in Fig. 6, and is represented by the blue dotted line, together with the average of the experimental results (red dots).

As seen in Fig. 6, from t = 9 h the experimental and numerical results present good correlation. This is because after the first nine hours of drying, the main process of liquid transport is no longer due to gravitational effect. The drying rate becomes considerably slower and capillary conduction and surface diffusion become the main processes of liquid transport. These are adequately simulated in WUFI. At t = 456 h, $\psi$(t) has a value of 7.0 kg/m$^3$. This value is closely related to the material water content at 95% RH, below which material water content is mostly in the vapour state.

## 5 CONCLUSIONS

Although MD ICB may be used as an external thermal insulating system, it is crucial importance to understand its behaviour when exposed to rain. An experimental study to evaluate the drying behaviour of MD ICB boards after wetting was performed. Its results were compared with those obtained by numerical simulation using WUFI 2D 3.0.

It was experimentally observed that, in the first nine drying hours the MD ICB boards lose water mass at a very high rate. Fifty-three percent of the initial water content is lost during this period, in which the movement of the liquid is mainly due to gravity. After this initial time, the drying process becomes considerably slower. The means of water transport considered in the simulation program, WUFI 2D 3.0, are capillary conduction and surface diffusion for liquid water transport. Additionally, the vapour diffusion and solution diffusion were also simulated. After the first nine hours it was found that the numerical and experimental results present a good correlation. Both liquid and vapour phase simulation have a good agreement with the real material drying behaviour. Thus, the material moisture content can be properly estimated when applied to a building as an external insulation coating material.

## ACKNOWLEDGEMENTS

The first author, Rosário Fino is grateful for the financial support provided by FCT (Fundação para a Ciência e Tecnologia), under the program MIT Portugal - Sustainable Energy Systems, through the doctoral degree grant SFRH/BD/52303/2013. This work has also been framed under the Energy for Sustainability Initiative of the University of Coimbra and is supported by the greenURBANLIVING Project (POCI-01-0247-FEDER-003393).

## REFERENCES

[1] Karade, S.R., Irle, M.A. & Maher, K., Physico-chemical aspects of the use of cork in cimentious composites. In *ICWSF 2001- The Fifth International Conference on the Development of World Science*, *Wood Technology and Forestry,* Ljubljana, Slovenia, pp. 97–106, 2001.

[2] Gil, L., Insulation corkboard for sustainable energy and environmental protection. *Ciência & Tecnologia dos Materiais,* **25**, pp 38–41, 2013.

[3] Luis, G., Cortiça: produção, tecnologia e aplicação, 1998.

[4] Silva, S.P., Sabino, M.A., Fernandes, E.M., Correlo, V.M., Boesel, L.F. & Reis, R.L., Cork: properties, capabilities and applications. *International Materials Reviews,* **50**, pp. 345–365, 2005.
http://dx.doi.org/10.1179/174328005X41168

[5] Gil, L. & Cortiço, P., Characterization of insulation corkboard obtained from demolitions. *Ciência & Tecnologia dos Materiais,* **23**, 2011.

[6] Jerman, M. & Černý, R., Effect of moisture content on heat and moisture transport and storage properties of thermal insulation materials. *Energy and Buildings,* **53**, pp 39–46, 2012.
http://dx.doi.org/10.1016/j.enbuild.2012.07.002

[7] Moon, H.J., Ryu, S.H. & Kim, J.T., The effect of moisture transportation on energy efficiency and IAQ in residential buildings. *Energy and Buildings,* **75**, pp. 439–446, 2014.
http://dx.doi.org/10.1016/j.enbuild.2014.02.039

[8] Chen, Z.Q. & Shi, M.H., Study of heat and moisture migration properties in porous building materials. *Applied Thermal Engineering,* **25**, pp 61–71, 2005.
http://dx.doi.org/10.1016/j.applthermaleng.2004.05.001

[9] Jelle, B.P., Traditional, state-of-the-art and future thermal building insulation materials and solutions – properties, requirements and possibilities. *Energy and Buildings,* **43**, pp. 2549–2563, 2011.
http://dx.doi.org/10.1016/j.enbuild.2011.05.015

[10] Srinivasan, K. & Wijeysundera, N.E., Heat and moisture transport in wet cork slabs under temperature gradients. *Building and Environment,* **36**, pp. 53–57, 2001. http://dx.doi.org/10.1016/S0360-1323(99)00068-2
[11] ISO 10051:2008 Thermal insulation - Moisture effects on heat transfer - Determination of a thermal transmissivity of a moist material, 2008.
[12] Peuhkuri, R., Rode, C. & Hansen, K.K., Non-isothermal moisture transport through insulation materials. *Building and Environment,* **43**, pp. 811–822, 2008. http://dx.doi.org/10.1016/j.buildenv.2007.01.021
[13] WUFI 2D 3.0. Fraunhofer Institut Bauphysik.
[14] EN 1602:2013 Thermal insulation products for building applications- Determination of the apparent density, 2013.
[15] NP EN 1936:2008 -Métodos de ensaio para pedra natural. Determinação das massas volúmicas real e aparente e das porosidades total e aberta, 2008.
[16] EN 12667:2012 - Thermal performance of building materials and products. Determination of thermal resistance by means of guarded hot plate and heat flow meter methods. Products of high and medium thermal resistance, 2012.
[17] EN 12086:2013- Thermal insulation for building applications - Determination of water vapour transmission properties, 2013.
[18] EN ISO 15148: 2012 Hygrothermal performance of building materials and products- Determination of water absorption coefficient by partial immersion, 2012.
[19] ISO 12571:2013- Higrothermal performance of building materials and products - Determination of hygroscopic sorption properties, 2013.
[20] Künzel, H.M., *Simultaneous Heat and Moisture Transport in Building Components One - and Two-dimensional Calculation using Simple Parameters*, IRB Verlag, 1995.
[21] Torres, M.I.M., PhD Thesis Humidade ascensional em paredes de construções históricas, 2004.